

# Thermally Stable Ge/Cu/Ti Ohmic Contacts to n-type GaN

NADEEMULLAH MAHADIK,<sup>1</sup> MULPURI V. RAO,<sup>1,3</sup> and ALBERT V. DAVYDOV<sup>2</sup>

1.—Department of Electrical and Computer Engineering, George Mason University, Fairfax, VA 22030.

2.—Materials Science and Engineering Laboratory, National Institute of Sciences and Technology, Gaithersburg, MD 20899. 3.—E-mail: rmulpuri@gmu.edu

The performance of a novel Ge/Cu/Ti metallization scheme on n-type GaN has been investigated for obtaining thermally and electrically stable low-resistance ohmic contacts. Isochronal (2 min.) anneals in the 600–740°C temperature range and isothermal (690°C) anneals for 2–10 min. duration were performed in inert atmosphere. For the 690°C isothermal schedule, ohmic behavior was observed after annealing for 3 min. or longer with a lowest contact resistivity of  $9.1 \times 10^{-5} \Omega \text{ cm}^2$  after the 10 min. anneal for a net donor doping concentration of  $9.2 \times 10^{17} \text{ cm}^{-3}$ . Mean roughness ( $R_a$ ) for anneals at 690°C was almost constant at around 5 nm, up to an annealing duration of 10 min., which indicates a good thermal stability of the contact scheme.

**Key words:** Ohmic contacts, GaN, metallization

## INTRODUCTION

Gallium nitride is the subject of extensive research for making commercial ultraviolet (UV)-blue light sources,<sup>1,2</sup> high-power microwave devices,<sup>3</sup> and high-temperature electronics.<sup>4</sup> Realization of low-resistivity ( $\rho_c$ ), thermally stable ohmic contacts is vital for high performance device applications.<sup>5</sup> Because the Fermi level on the GaN surface is unpinned,<sup>6</sup> ohmic contacts for n-type GaN can be formed by selecting a metal whose work function is less than the electron affinity of GaN, or by increasing donor concentration at the GaN surface to invoke tunneling. There are numerous reports<sup>7–26</sup> on developing and optimizing ohmic contacts to n-type GaN. Traditionally, contact schemes with titanium metal as the first layer have been most widely used.<sup>8–11,15,22</sup> Ti is selected as the first contact layer to n-type GaN because its work function, 4.33 eV, is close to that of n-GaN (electron affinity = 4.1 eV). Ohmic behavior of a GaN/Ti system has been attributed to the out-diffusion of nitrogen from the GaN into the Ti, creating N vacancies, which act as donors at the GaN surface.<sup>8,10,11,22</sup> The introduction of excess donors at the metal/n-GaN interface causes carrier tunneling through the thin metal/semiconductor barrier, which results in an ohmic behavior to the contact system. Ti is also known to reduce native oxide on the GaN surface, thus promoting more intimate metal-to-GaN contact. Hence,

a Ti layer at the metal-contact/GaN interface has proved beneficial and is currently used in most of the contact schemes.

In this work, we investigated the Cu-based scheme as an alternative to commonly used Au, Al-containing metallization (e.g., Au/Al/Ti) for forming ohmic contacts to n-GaN. To our knowledge, there has been only one report<sup>24</sup> on copper-based ohmic contacts to n-type GaN, with annealing performed at 400°C for a prolonged time, and one report<sup>25</sup> on forming Cu<sub>3</sub>Ge-based Schottky contact to n-type GaN at a much higher annealing temperature. This ambiguity in metallization composition, annealing temperature, and time needs to be investigated. Also, there have been a few reports<sup>26,27</sup> on copper-based ohmic contacts to p-type GaN. If Cu-based low-resistivity contacts can also be developed for n-type GaN, then ohmic contacts to both n- and p-type regions in GaN-based device structures can be formed concurrently in the same process. Because the work function of copper is greater than the electron affinity of GaN (4.65 eV and 4.1 eV, respectively), Cu should not produce an ohmic contact due to the barrier at the Cu/n-GaN interface. To create ohmic contacts to n-GaN, a metal with a lower work function, such as Ti, needs to be used as the first layer. Germanium, which is predominantly a donor impurity in III-V compounds, can be added to the ohmic contact metal system to invoke tunneling at the metal/n-GaN contact. In this work, we have selected the Ge/Cu/Ti metal scheme with the thickness of Ge and Cu layers

corresponding to 1:3 Ge/Cu atomic ratio. The rationale for choosing 1:3 ratio was due to desired formation of  $\epsilon_1$ -intermetallic  $\text{Cu}_3\text{Ge}$  phase, which has advantages such as low temperature of formation, low electrical resistivity, high oxidation resistance, and high thermal stability.<sup>28–30</sup>

## EXPERIMENTAL PROCEDURE

The 7  $\mu\text{m}$  thick n-GaN epilayers, grown by hydride-vapor phase epitaxy (HVPE) on a 2 in. sapphire (0001) substrate, were obtained commercially. Hall measurements yielded a mobility of 197  $\text{cm}^2 \text{V}^{-1} \text{s}^{-1}$  at 300 K, and a net donor concentration of  $9.2 \times 10^{17} \text{cm}^{-3}$ . The wafer surface preparation was performed using a standard RCA procedure. Circular transmission line model (c-TLM) patterns with an inner diameter of 120  $\mu\text{m}$  and variable outer diameters of 122–184  $\mu\text{m}$  were formed using standard e-beam deposition and lift-off photolithography. Three metallization schemes were fabricated. Their compositions and annealing schedules are summarized in Table I. Contact annealing was performed in commercial rapid thermal annealing (RTA) system in ultra-high purity (UHP)-grade argon, which was additionally gettered to remove residual oxygen and moisture. Selection of three annealing temperatures—600°C, 690°C, and 740°C—was guided by the thermal stability ranges of the  $\text{Cu}_3\text{Ge}$  phase, which exists in three structural modifications,  $\epsilon_1$ ,  $\epsilon_2$ , and  $\epsilon_3$ ,<sup>31</sup> and was expected to form in all proposed metallization schemes from Table I. The annealing temperature of 600°C was chosen just to be below the 636°C peritectoid decomposition of  $\epsilon_1$ - $\text{Cu}_3\text{Ge}$  compound; 690°C was chosen to be below the 698°C peritectic decomposition of  $\epsilon_2$ - $\text{Cu}_3\text{Ge}$  compound; and 740°C was selected to be below the 747°C melting temperature of the  $\epsilon$ - $\text{Cu}_3\text{Ge}$  phase (see phase diagram in Ref. 31).

Current-voltage (I-V) and specific contact resistivity measurements were made using a four-point probe arrangement for the circular TLM patterns, as described in Marlow and Das.<sup>32</sup> Contact surface morphology was investigated by field emission scanning electron microscopy (FESEM) using a Hitachi-4700 system. The surface morphology was also assessed by atomic force microscopy (AFM) on 5  $\mu\text{m} \times 5 \mu\text{m}$  and 50  $\mu\text{m} \times 50 \mu\text{m}$  areas using a Veeco AFM system. Auger electron spectroscopy (AES)

was performed commercially to obtain the compositional depth profile. Phase analysis was conducted by x-ray diffraction on Bruker-AXS D8 general area detector diffraction system (GADDS) with Cu  $K_\alpha$  radiation.

## RESULTS AND DISCUSSION

### I-V Characteristics

The first two metallization schemes (Cu/Ge/Ti) from Table I yielded nonohmic contacts even for alloying temperatures as high as 740°C. Nonlinearity had somewhat decreased for a metallization scheme with a thicker (25 nm) Ti layer compared to a 10 nm Ti layer. Nonlinear behavior could be due to unintentional oxidation of the Cu surface layer (greenish discoloration of the contact surface was observed for the annealed samples) that occurred prior to Cu and Ge intermixing. Ohmic behavior was observed for the third metallization scheme in Table I, Ge (40 nm)/Cu (70 nm)/Ti (25 nm), in which the order of Cu and Ge layers was switched. The I-V curves for the isothermal anneals at 690°C and for 600°C / 2 min. anneal are shown in Fig. 1a for a 32  $\mu\text{m}$  contact separation in the TLM pattern. The contacts showed a highly rectifying behavior for 600°C / 2 min. annealing. For an anneal at 690°C for 2 min., the rectifying behavior decreased notably. For the 3 min. annealing at 690°C the contacts turned ohmic. The contacts remained ohmic for longer annealing times with decreasing specific contact resistivity,  $\rho_c$ . Figure 1b shows the specific contact resistivities for annealing times  $\geq 3$  min. at 690°C. The  $\rho_c$  decreased with increasing annealing time reaching a value of  $9.1 \times 10^{-5} \Omega\text{-cm}^2$  for 10 min. annealing. The surface morphology of contacts annealed at 690°C remained smooth with a roughness of  $\sim 5$  nm and did not deteriorate with increasing annealing time, as illustrated later by the AFM surface roughness data. The anneal performed at 740°C yielded very poor surface morphology (shown later in Fig. 5c) for performing any reliable electrical measurements. The TLM patterns often shorted due to partial melting of the contact (evident from the inset of Fig. 5c), which resulted in unreliable I-V characteristics. In fact, partial melting of the contact at 740°C was anticipated from the Cu-Ge phase diagram, since this temperature is inside of the 698–747°C interval, in which  $\epsilon$ - $\text{Cu}_3\text{Ge}$  coexists with a liquid phase.<sup>31</sup> In other words, 698°C is an upper limit of thermal stability of any  $\text{Cu}_3\text{Ge}$ -based metallization; above this temperature, partial ( $\leq 747^\circ\text{C}$ ) or complete ( $> 747^\circ\text{C}$ ) melting is expected.

### AES Depth Profiles

The AES depth profiles of the Ge/Cu/Ti/GaN system (Fig. 2) depict the intermixing of the various metals for different annealing conditions. The GaN/Ti interface reaction occurred with the annealing at 690°C for 2–10 min. Ti profiles in Fig. 2b–d

**Table I. Annealing Schemes Used for the Metals Deposited on n-GaN Epilayers under Continuous Ultra-High Purity Argon Purging**

	Metallization scheme	Annealing (Temperature/Time)
1	Cu (70 nm)/Ge (40 nm)/Ti (10 nm)	600°C/2 min, 740°C/1 min
2	Cu (70 nm)/Ge (40 nm)/Ti (25 nm)	600°C/2 min, 740°C/1 min
3	Ge (40 nm)/Cu (70 nm)/Ti (25 nm)	600°C/2 min, 690°C/2,3, 5,10 min, 740°C/2 min

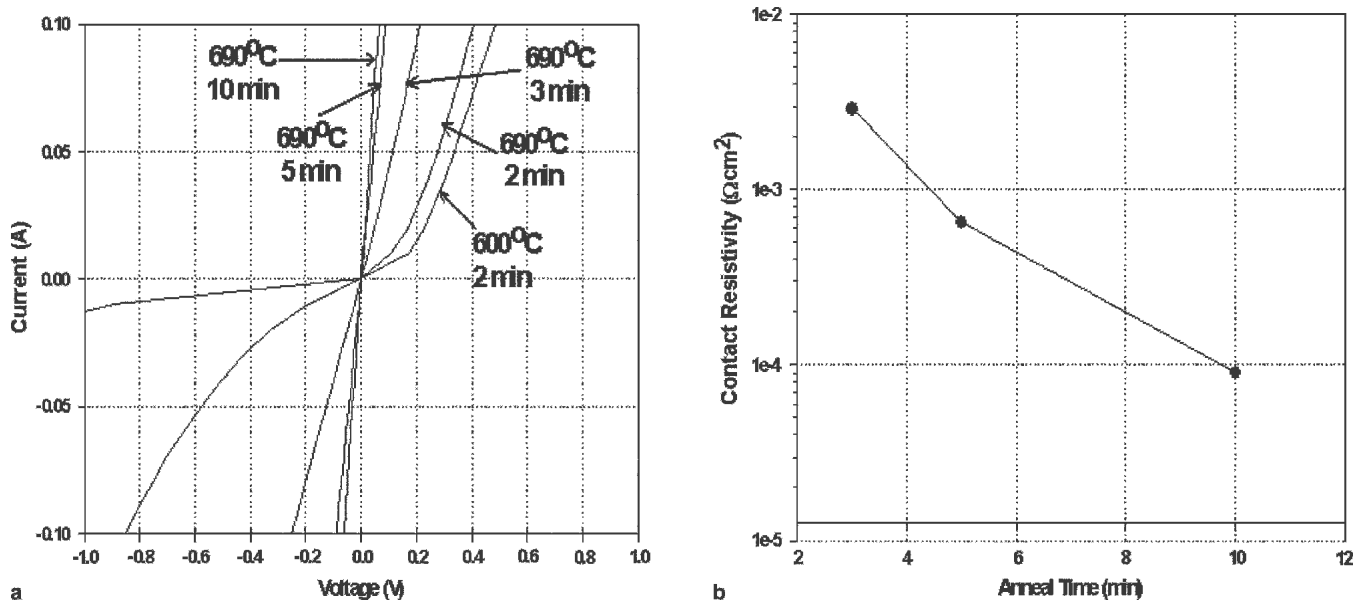


Fig. 1. (a) I-V curves of the Ge/Cu/Ti metal system for the 32  $\mu\text{m}$  contact separation for different annealing temperatures and times. (b) Variation of specific contact resistivity with annealing time at 690°C annealing temperature.

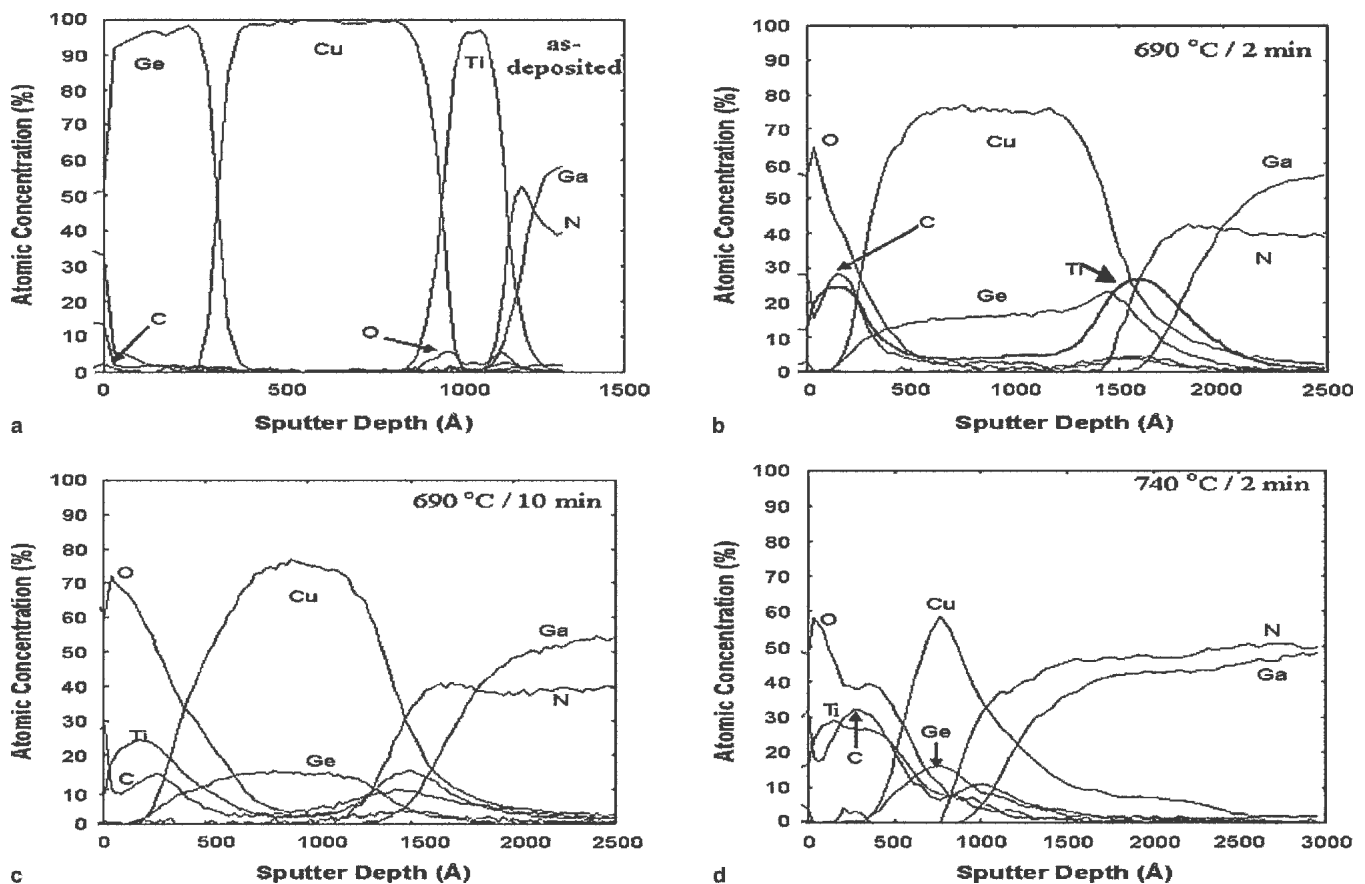


Fig. 2. AES depth profiles of the Ge (40 nm)/Cu (70 nm)/Ti (25 nm)/GaN system for as-deposited and annealed samples: (a) as deposited, (b) 690°C / 2 min., (c) 690°C / 10 min., and (d) 740°C / 2 min.

shows that part of the Ti remained at the GaN interface while another part out-diffused to the surface. Overlap of Ti and N concentration profiles in the vicinity of the GaN interface indicates their inter-

mixing and possible formation of the titanium nitride phase. It is believed that formation of a thin  $\text{TiN}_x$  layer at the metal/GaN interface results in N vacancy (a donor in GaN) creation at the GaN

surface, which enhances the ohmic behavior of the contact.

In the metal layers, Ge intermixed with Cu even after the shortest (2 min.) annealing at 690°C (Fig. 2b). The Ge and Cu profiles in Figs. 2b–2d match with roughly 3:1 Cu to Ge atomic ratio indicating formation of the  $\epsilon_1$ -Cu<sub>3</sub>Ge phase. The Ge and Cu did not undergo any prominent reaction with the other elements present in the system, which shows the stability of the Cu<sub>3</sub>Ge phase. At higher temperatures (740°C), a significant intermixing between all the elements is observed because of partial or complete melting of the  $\epsilon$ -Cu<sub>3</sub>Ge phase.<sup>31</sup> Potential diffusion of small amount of Ge into GaN may have also contributed to ohmic behavior because of predominantly donor behavior of amphoteric Ge in III-V compounds.<sup>28</sup>

In addition, a high level of oxygen can be clearly seen at the surface of annealed samples (Figs. 2b–2d), which was not observed in the as-deposited sample (Fig. 2a). An increase in the level and thickness of penetration of the O is observed at the metal surface with increasing annealing time or temperature. The oxygen is believed to have entered the metal system from the annealing ambient in which its concentration is in the parts-per-million range. The O and Ti profiles on the surface roughly followed the same shape with a higher O concentration than the Ti, which is indicative of titanium oxide formation. The presence of titanium oxide on the surface may possibly lead to a slight increase in  $\rho_c$  and  $R_a$ .

The AES depth profiles did not show any evidence of copper or germanium oxide formation on the surface of the contacts, which indicates a resistance of the Cu<sub>3</sub>Ge phase to oxidation.

## X-ray

Figure 3 shows the x-ray data for as-deposited (Fig. 3a) and annealed (Figs. 3b–3d) samples. The as-deposited sample contains Ti and Cu phases with strong (0002) and (111) preferred orientation, respectively. Germanium peaks were not detected, possibly due to the germanium layer being thin and/or having no texture. After annealing at 600°C and above, the Ti and Cu peaks disappeared, indicating complete reaction of the metals, which agrees with AES results in Fig. 2b–2d. New peaks on XRD scans in Fig. 3b–3d correspond to the  $\epsilon_1$ -Cu<sub>3</sub>Ge orthorhombic phase. Its lattice parameters varied with annealing temperature/time due to possible change of the Cu<sub>3-x</sub>Ge composition. From the scan in Fig. 3, the  $\epsilon_1$ -Cu<sub>3</sub>Ge lattice parameters were determined as follows: sample (b)  $a = 5.163(6)$  Å,  $b = 4.177(4)$  Å,  $c = 4.446(4)$  Å; sample (c)  $a = 5.175(3)$  Å,  $b = 4.179(2)$  Å,  $c = 4.455(2)$  Å; and sample (d)  $a = 5.223(3)$  Å,  $b = 4.185(2)$  Å,  $c = 4.489(2)$  Å. For comparison, values for the  $\epsilon_1$ -Cu<sub>3</sub>Ge polycrystalline phase from Ref. 33 are slightly larger,  $a = 5.29$  Å,  $b = 4.20$  Å,  $c = 4.55$  Å, which could be attributed to the compositional difference between thin films from the present work

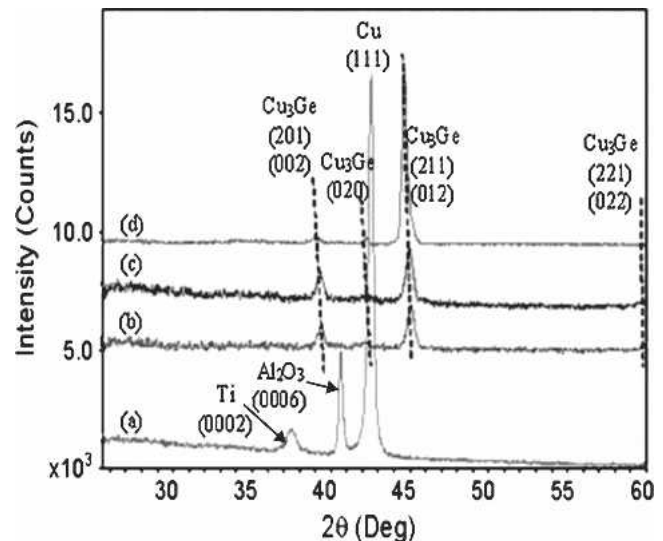


Fig. 3. XRD spectra for (a) as deposited, (b) 600°C / 2 min., (c) 690°C / 2 min., and (d) 740°C / 2 min. anneals. The  $\epsilon_1$ -Cu<sub>3</sub>Ge (Pearson symbol *oP8*) phase was formed in samples (b), (c), and (d); peaks for this phase are marked with dotted lines for eye-guiding purpose only.

and bulk sample from Ref. 33. A noteworthy feature of Fig. 3 is a drastic increase in the intensity of the 211 peak for sample (d) (740°C/2 min. anneal) as compared to samples annealed at lower temperatures. Strong (211) preferred orientation in sample (d) could be associated with recrystallization from the melt, which was likely present at 740°C (as discussed in the I-V Characteristics section above), as opposed to solid-type transformations at 600°C and 690°C annealing conditions.

No TiN peaks were detected for the annealed samples even though the formation of this phase was inferred from the Auger analysis (see Figs. 2b–2d). The absence of TiN peaks on XRD scans could be explained by the fact that TiN is likely to be very thin and is buried under a thick  $\epsilon_1$ -Cu<sub>3</sub>Ge layer.

## AFM Results

AFM scans were taken for the Ge/Cu/Ti metallizations for the 2 min. duration isochronal anneals at 600–740°C, and for the same metallization for the 690°C isothermal anneals of 2–10 min. duration. The root-mean-square (rms) roughness ( $R_a$ ) is shown in Fig. 4 for both isochronal (Fig. 4a) and isothermal (Fig. 4b) anneals. Drastic increase of  $R_a$  after annealing at 740°C (Fig. 4a) is likely associated with partial melting of the  $\epsilon$ -Cu<sub>3</sub>Ge phase. Mean roughness values of 4–6 nm remained unchanged after anneals at 600°C and 690°C, even after prolonged (10 min.) annealing time, which indicates thermal stability of the  $\epsilon_1$ -Cu<sub>3</sub>Ge phase and of the metal contact as a whole.

## FESEM Images

FESEM images for the 690°C isothermal anneals and 740°C/2 min. anneals are shown in Fig. 5a–c.

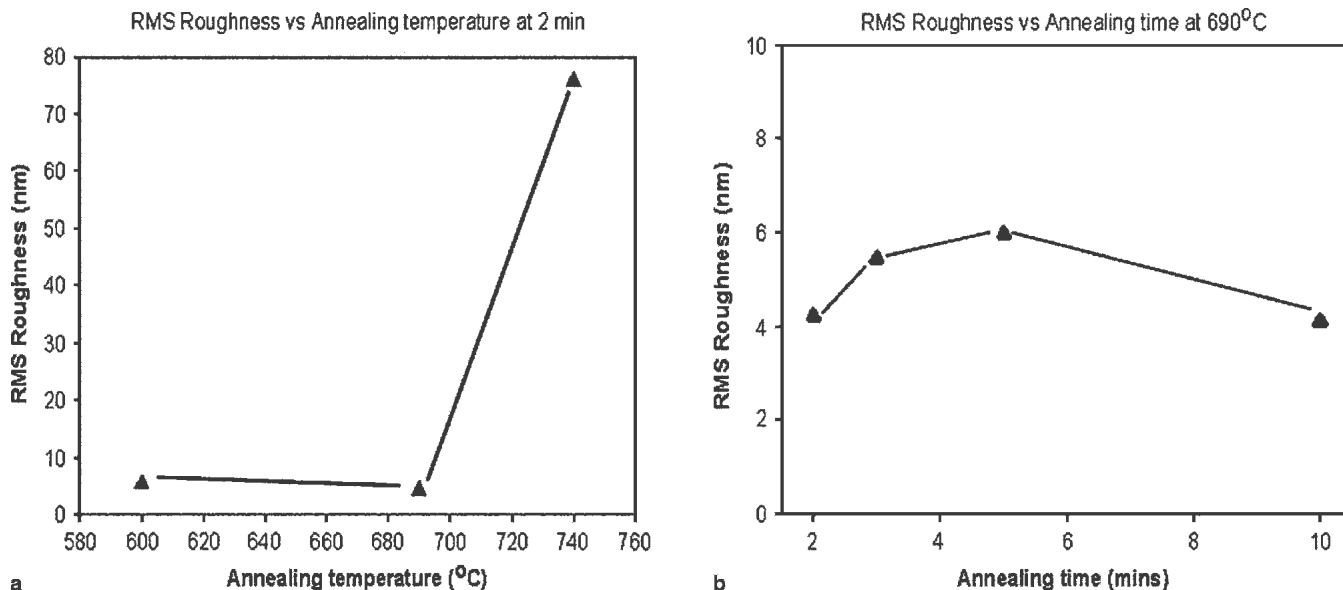


Fig. 4.  $R_a$  vs. (a) anneal temperature for 2 min. anneals and (b) anneal time for 690°C anneals.

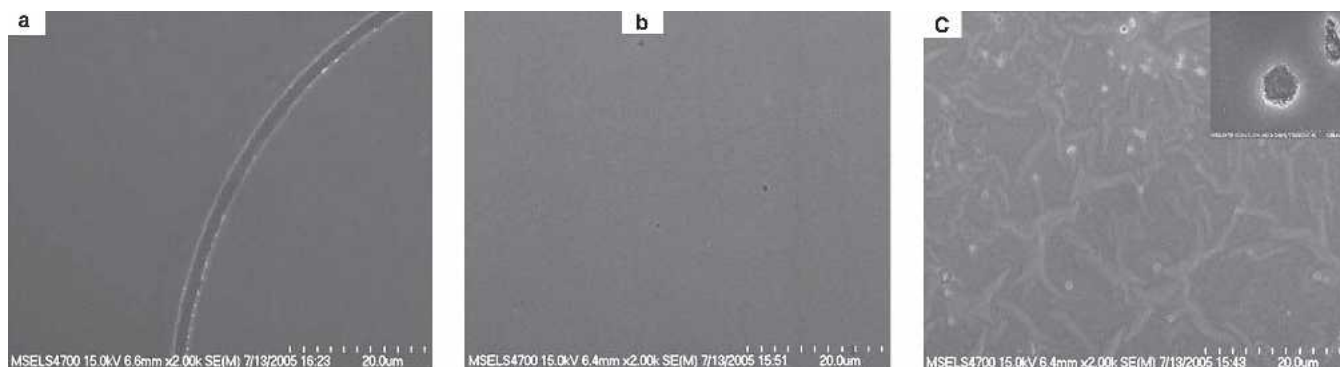


Fig. 5. FESEM images of samples after annealing at (a) 690°C for 5 min., (b) 690°C for 10 min., and (c) 740°C for 2 min. Images were acquired at 2 k magnification; inset in (c) was acquired at 40 k magnification.

The surface of the sample annealed at 600°C was smooth (not shown) and did not show any sign of surface deterioration. The contact surfaces after isothermal 690°C anneals were also smooth with slight increase in roughness with increased annealing time (Figs. 5a–5b). The sample annealed at 740°C for 2 min. (Fig. 5c) showed prominent degradation of the contact surface, which correlates with AFM observations. As indicated above, this deterioration is likely associated with partial melting of the contact at the 740°C annealing temperature.

## CONCLUSIONS

In this work, a novel thermally stable low resistive Ge/Cu/Ti ohmic contact to n-type GaN has been fabricated. The minimum  $\rho_c$  was found to be  $9.1 \times 10^{-5} \Omega\text{-cm}^2$  after a 690°C/10 min. anneal for a GaN layer doped with a net donor concentration of  $9.2 \times 10^{17} \text{ cm}^{-3}$ . The contact surface remained smooth after 690°C anneals, practically independent of the annealing time with mean roughness of  $5 \pm 1 \text{ nm}$ . The anneal at a lower temperature of 600°C was rendered nonohmic. The anneal at a higher temper-

ature of 740°C produced a morphologically degraded metallic film with high ( $R_a = 29 \text{ nm}$ ) surface roughness, which can be attributed to partial melting in the Cu-Ge system. The  $\epsilon_1\text{-Cu}_3\text{Ge}$  phase formed as a result of RTA was found to be oxidation resistant and thermally stable even after prolonged (10 min.) annealing time at 690°C. Comparison of our results with recently reported<sup>34,35</sup> values indicates that the surface roughness of the metal contact from this study is superior to those reported in the literature. This is believed to be due to the lower annealing temperature required to realize the ohmic behavior for the metallization used in this study and good thermal stability of the  $\epsilon_1\text{-Cu}_3\text{Ge}$  phase. However, our contact resistance values are higher due to a lower doping concentration of GaN used in the current study, which plays an important role in the value of contact resistance.

## ACKNOWLEDGEMENTS

This work is supported by the National Science Foundation (NSF) under Grant No. ECS-0330226 and by Army Research Office (Dr. Prater) under

Grant No. W911NF-04-1-0428. Facilities at the National Institute of Sciences and Technology (NIST) were used. The authors would like to thank A. Motayed, a graduate student of the University of Maryland, for his help with the contact resistivity measurements and valuable discussions. Certain commercial instruments are identified in this paper in order to specify the experimental procedure adequately and do not imply endorsement by NIST.

## REFERENCES

1. S. Nakamura, M. Senoh, N. Iwasa, and S.I. Nagahama, *Appl. Phys. Lett.* **67**, 1868 (1995).
2. S. Nakamura, M. Senoh, S.I. Nagahama, N. Iwasa, T. Yamada, T. Matsushita, H. Kiyoku, and Y. Sugimoto, *Jpn. J. Appl. Phys.* **35**, L74 (1996).
3. H. Morkoc, S. Strite, G.B. Gao, M.E. Lin, B. Sverdlov, and M. Burns, *J. Appl. Phys.* **76**, 1363 (1994).
4. *High Temperature Electronics*, ed., F.P. McCluskey, R. Grzybowski, and T. Podlesak (Cleveland, OH: CRC Press, 1997).
5. P.H. Holloway, T.J. Kim, J.T. Trexler, S. Miller, J.J. Fijol, W.V. Lampert, and T.W. Haas, *Appl. Surf. Sci.* **117/118**, 362 (1997).
6. S.C. Binari, H.B. Dietrich, G. Kelner, L.B. Rowland, K. Doverspike, and D.K. Gaskill, *Electron. Lett.* **30**, 909 (1994).
7. J.S. Foresi and T.D. Moustakas, *Appl. Phys. Lett.* **62**, 2859 (1993).
8. M.E. Lin, Z. Ma, F.Y. Huang, Z.F. Fan, L.H. Allen, and H. Markoc, *Appl. Phys. Lett.* **64**, 1003 (1994).
9. A.I. Ping, M.A. Khan, and I. Adesida, *J. Electron. Mater.* **25**, 819 (1996).
10. Z. Fan, S.N. Mohammed, W. Kim, O. Aktas, A.E. Botchkarev, K. Duxstad, and E.E. Haller, *J. Electron. Mater.* **25**, 1703 (1996).
11. L.F. Lester, J.M. Brown, J.C. Ramer, L. Zhang, S.D. Hersee, and J.C. Zolper, *Appl. Phys. Lett.* **69**, 2737 (1996).
12. S. Miller and P.H. Holloway, *J. Electron. Mater.* **25**, 1709 (1996).
13. D.B. Ingerly and Y.A. Chang, *Appl. Phys. Lett.* **70**, 108 (1997).
14. J. Burm, K. Chu, W.A. Davis, W.J. Schaff, and T.J. Eustis, *Appl. Phys. Lett.* **70**, 464 (1997).
15. B.P. Luther, S.E. Mohny, T.N. Jackson, M.A. Khan, Q. Chen, and J.W. Wang, *Appl. Phys. Lett.* **70**, 57 (1997).
16. Y.-F. Wu, W.-N. Jiang, B.P. Keller, S. Keller, D. Kapolnek, S.P. Denbaars, U.K. Mishra, and B. Wilson, *Solid-State Electron.* **41**, 165 (1997).
17. H. Cordes and Y.A. Chang, *MRS Internet J. Nitride Semicond. Res.* **2**, 2 (1997).
18. E. Kaminska, A. Piotrowska, M. Guziewicz, S. KasjaNiuk, A. Barcz, E. Dynowska, M.D. Bremser, O.H. Nam, and R.F. Davis, *Mater. Res. Soc. Symp. Proc.* **449**, 1055 (1997).
19. S.E. Mohny, B.P. Luther, S.D. Wolter, T.N. Jackson, R.F. Karlicek, Jr., and R.S. Kern, *Proc. 4th Int. High Temp. Electron. Conference*, Albuquerque, NM (Piscataway, NJ: IEEE, 1998), p. 134.
20. S.J. Pearton, S.M. Donovan, C.R. Abernathy, F. Ren, J.C. Zolper, M.W. Cole, A. Zeitouny, M. Eizenberg, and R.J. Shul, in Ref. 19, p. 296.
21. N.A. Papanicolaou, A. Edwards, M.V. Rao, J. Mittereder, and W.T. Anderson, *J. Appl. Phys.* **87**, 380 (2000).
22. D.-F. Wang, F. Shiwei, C. Lu, A. Motayed, M. Jah, S.N. Mohammad, K.A. Jones, and L. Salamanca-Riba, *J. Appl. Phys.* **89**, 6214 (2001).
23. S.-C. Lee, J.-C. Her, S.-M. Han, K.-S. Seo, and M.-K. Han, *Electrochem. Solid-State Lett.* **8**, G135 (2005).
24. J.-H. Chern, L. P. Sadwick, and R.J. Hwu, in Ref. 19, p. 114.
25. H.-C. Hsin, W.-T. Lin, J.R. Gong, and Y.K. Fang, *J. Mater. Sci. Mater. Electron.* **13**, 203 (2002).
26. S.H. Liu, J.M. Hwang, Z.H. Hwang, W.H. Hung, and H.L. Hwang, *Appl. Surf. Sci.* **212–213**, 907 (2003).
27. J. Song, J.S. Kwak, and T. Seong, *Appl. Phys. Lett.* **86**, 062103 (2005).
28. M.O. Aboelfotoh, K.N. Tu, F. Nava, and M. Michelini, *J. Appl. Phys.* **75**, 1616 (1994).
29. M.O. Aboelfotoh, C.L. Lin, and J.M. Woodall, *Appl. Phys. Lett.* **65**, 3245 (1994).
30. Z. Wang, G. Ramanath, L.H. Allen, A. Rockett, J.P. Doyle, and B.G. Svensson, *J. Appl. Phys.* **82**, 3281 (1997).
31. T.B. Massalski, *Binary Alloy Phase Diagrams*, 2nd ed. (Materials Park, OH: ASM International, 1990).
32. G.S. Marlow and M.B. Das, *Solid-State Electron.* **25**, 91 (1982).
33. Powder Diffraction File No. 65-2590 (Newtown Square, PA: JCPDS International Centre for Diffraction Data, 1998).
34. D. Selvanathan, F.M. Mohammed, A. Tesfayesus, and I. Adesida, *J. Vac. Sci. Technol. B* **22**, 2409 (2004).
35. V. Reddy, S. Kim, and T.Y. Seong, *J. Electron. Mater.* **33**, 395 (2004).